ROYAL SOCIETY OF CHEMISTRY

PAPER

Check for updates

Pyridinium-furfuryl-modified granular agro-waste adsorbent for orthophosphate recovery

Bernd G. K. Steiger [ID] and Lee D. Wilson [ID] *

In this study, a granular composite comprised of 50% oat hulls (Oh), 10% kaolinite (K), and 40% modified chitosan (Chi) was crosslinked with epichlorohydrin (ECH) and subsequently functionalized with pyridinium. The modified Chi was obtained through synthetic conversion of a furfural-moiety attached *via* the amine-groups of chitosan (Oh50−Furfural). For comparison, non-modified pellets (Oh50), NaOH-neutralised pellets (Oh50−NaOH) and ECH crosslinked composites (Oh50−ECH) were used to elucidate the effect of variable synthetic modification. An analysis of the ^{13}C solids NMR spectral results for the Oh50−Furfural composite revealed the presence of a product mixture, both chitosan with imine-linked furfuryl- and pyridinium moieties. Experimental support by infrared spectroscopy and thermogravimetric analysis corroborate the modified structure of Chi. Although the absolute orthophosphate adsorption capacity was low (5 mg g^{-1} at pH 4.75 and 1 mg g^{-1} at pH 8.5), the furfuryl-pyridinium modified adsorbent showed pH independent adsorption, which is in contrast to non-modified chitosan-based composites that often require acidic media. This study demonstrates that composites containing agro-waste and chitosan can be synthetically modified to incorporate pyridinium-moieties (alongside furfuryl-moieties) to enhance the adsorption properties towards orthophosphate, especially at low concentrations and neutral or slightly alkaline pH.

Sustainability spotlight

Agricultural effluents and wastewaters with orthophosphate (P$_i$) present a global challenge due to eutrophication. Remediation of low P$_i$ concentrations (*ca.* 5 mg L^{-1}) still present challenges, especially at environmentally relevant pH conditions. This research uses a sustainable synthetic pathway to modify chitosan with suitable properties as an additive within granular biomass composites. The unique properties of the prepared composites over other conventional chitosan-based adsorbents are revealed in this research. The facile and sustainable approach described herein is suitable for scale-up and implementation in current water treatment technologies for the sustainable treatment of orthophosphate laden waters. Our work emphasizes the importance of the following UN sustainable development goals: water and sanitation (SDG 6); industry, innovation and infrastructure (SDG 9).

Introduction

With increasing water stress induced through climate change and increasing anthropogenic activities, safeguarding access to potable water is an increasingly important water security issue. To fulfil the UN Sustainable Development Goal (UN SDG) related to clean water and sanitation, research of this type is a matter of increasingly global importance.[1] Orthophosphate (P$_i$) as a pollutant contributes to eutrophication, while its efficient removal from agricultural effluent and wastewater remains a current challenge.[2,3] The recovery of P$_i$ from surface waters will serve to address contamination and recovery of this valuable nutrient was further highlighted by Ung and Li[4] for the case of phosphate rock mining. Various current technologies for water treatment require significant infrastructure and operational costs (*e.g.*, reverse osmosis) or employ toxic

chemical agents such as heavy metal salts for precipitation-based removal that warrant further consideration from a sustainability viewpoint.[5,6] Adsorption-based removal offers a relatively low-cost and facile water treatment method with highly efficient contaminant removal, according to the nature of the adsorbent.[7–9]

Chitosan is a versatile biopolymer platform that has seen continued research interest for water treatment applications.[10,11] Chitosan is a polysaccharide derived from chitin,[12] which is comprised of the *N*-acetylglucosamine monomer unit. By comparison, chitosan is obtained from chitin *via* deacetylation, where a minimum of *ca.* 50% of the monomer units are converted to glucosamine units. The presence of abundant amine groups of chitosan enable facile chemical modification *via* Schiff base adducts with aldehydes, in contrast with more demanding synthetic conditions required for modification of cellulose. Research efforts directed at dye removal with low-cost and renewable adsorbents is a key topic of continued interest, where bio-sorbents are positioned to offer sustainable and cost-

Department of Chemistry, University of Saskatchewan, 110 Science Place, Saskatoon, S7N 5C9, Canada. E-mail: lee.wilson@usask.ca

effective water treatment.[13] In particular, the utilization of biomass waste materials for adsorbent preparation has garnered significant research interest to benefit local economies and facilitate an emerging global circular economy.[14–18] The valorization of agro-waste as adsorbent materials by employing biomass such as oat hulls and wheat straw waste for the removal of lead ions and methylene blue highlight the utility of such materials.[19,20] The compositing of a chitosan with agro-waste can yield a high-value product with lower input chemical costs, and enhanced adsorption properties with greater access to the active sites, according to synergistic effects reported for such materials.[21,22]

Biomass composites derived from spent coffee grounds or torrefied wheat straw have favourable stability in aqueous media, especially under acidic conditions *versus* non-torrefied biomass such as oat hulls.[20,23] As well, composites with greater oat hull content, especially above 40–60% display limited mechanical stability, as evidenced by crumbling in the dry state. Hardness of such composites in the dry state was measured around 20–30 N for non-crosslinked and *ca.* 60 N for crosslinked composites. Furthermore, these composites show susceptibility to breakdown in aqueous media with low salinity or slight acidity as outlined in previous research.[19,23] In turn, surface modification is required to reach acceptable mechanical strength and continued resilience in aqueous media for remediation applications in dynamic environments. For the case of aqueous media in many river systems, pH conditions reside near 7–8, where anion adsorption by chitosan can become attenuated or negligible.[24,25]

While chemical crosslinking addresses the aforementioned low mechanical strength and improves hydrostatic resilience, this introduces lower active site accessibility for adsorption and restricts expansion of the polymer network. Therefore reducing the adsorption capacity of the crosslinked composites. To also address the pH limitations of chitosan above pH 7, the surface of such crosslinked agro-waste pellets can be modified *via* cation incorporation to improve the adsorption properties.

An alternative strategy of introducing permanent cation species onto the chitosan backbone through quaternisation of the amine groups offers a unique alternative for conversion into pyridinium cations through furfural, which obviates the use of methyl iodide or other toxic reagents such as *N-2,4-dinitrobenzene pyridinium chloride*. Furfural can be derived from a variety of sugars through thermal dehydration, which presents a sustainable precursor that can be obtained without any fossil resources *via* a biorefinery approach.[26–33] Thus, the synthetic modification of the amine groups from chitosan to generate a permanent cation within the composite structure aims to improve the adsorption properties *versus* composites that contain unmodified chitosan.[34] The modification of chitosan was adapted from the synthesis of ionic liquids with furfural (*cf.* Scheme 1) as a proposed synthetic pathway.[31]

The pyridinium ion and formate/acetate as counterions are modelled after ion exchange resins that will afford their use in chitosan-based composites that contain oat hulls, which is a renewable and under-utilized biomass resource. This study outlines a *proof-of-concept* that such modifications are possible,
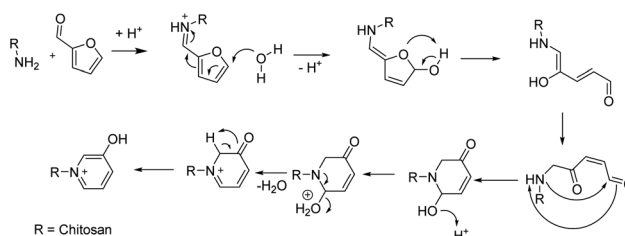
Scheme 1 Imine formation through reaction of chitosan with furfural and proposed subsequent acid catalysed ring-opening reaction with pyridinium formation (counterions omitted, potentially formate or acetate from the composite).[35] R is an alkyl group, which represent the C2 site of the glucosamine monomer unit of chitosan, as denoted in Fig. 2.

which will catalyse further research for a more sustainable synthetic route for modified biopolymer adsorbent systems *via* green and sustainable methods.

Materials and methods

Materials

Low molecular weight chitosan (deacetylation degree *ca.* 82%), kaolinite, KBr (IR-grade), epichlorohydrin (ECH) (99%+), potassium phosphate di-basic (ACS grade) and a ready-to-use vanadate–molybdate reagent (for phosphate determination, product# 108498) were purchased from Sigma-Aldrich (Oakville, Canada). Glacial acetic acid (99.7%), sodium hydroxide (97%), potassium phosphate mono-basic (ACS grade) and hydrochloric acid (36.5%) were purchased from Fisher Scientific (Ottawa, Canada). Formic acid (98%) was purchased from EMD (Merck, Darmstadt, Germany). Furfural (98%) was purchased from Merck (Darmstadt, Germany). Ethanol (100%) was acquired from Greenfield Global (Brampton, Canada). Oat hulls (Oh) were obtained from the College of Engineering (Richard Evitts) at the University of Saskatchewan. All chemicals were used without further purification. Millipore water (resistivity 18.2 MOhm) was used for all sample preparation.

Methods

Pellet preparation. Approximately 5 g of finely ground oat hulls (*ca.* 40–100 mesh) were combined with 1 g kaolinite and 4 g chitosan (10 g total) and mixed. 15–20 mL of 0.2 M AcOH was added and mixed until a uniform paste was obtained. Then, the paste was extruded through a glass syringe (*ca.* 5 mm opening). The extrudate was cut into *ca.* 4–8 mm long pellets and dried for
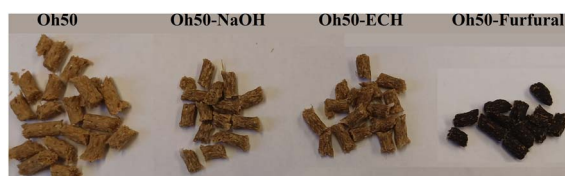

Fig. 1 Prepared composites from left to right: Oh50 (no NaOH), Oh50–NaOH, Oh50–ECH, and Oh50–Furfural.

18–24 h at *ca.* 22 °C. The dried pellets were divided into four equal weight fractions, *ca.* 2.25 g each (see also Fig. 1 for the appearance of the prepared composites).

Oh50. No further modification.

Oh50–NaOH. The dried pellets were added to 250 mL 1.8 M NaOH solution and stirred for 2 h, then left overnight at 23 °C. The pellets were washed with Millipore water until a neutral pH was attained.

Oh50–ECH. The dried Oh50 pellets were added to a 250 mL 1% ECH in 1.8 M NaOH solution, stirred for 2 h at 23 °C and then left overnight. The pellets were then washed with Millipore water until neutral pH was obtained and then air dried at 22 °C.

Oh50–Furfural. The dried pellets were crosslinked and washed according to the procedure described for the Oh50–ECH system. The washed pellets were added to *ca.* 125 mL 50% ethanol solution. 2.25 g pellets contain *ca.* 0.9 g chitosan (0.006 mol glucosamine monomer unit). 2 mol-eq. furfural (*ca.* 0.012 mol; 1.4 mL) and 0.3 mol-eq. formic acid (0.002 mol; 0.12 mL) were added and the mixture stirred for 3 d under reflux. Then, the pellets were washed until a neutral pH was met and dried at 22 °C for 24 h.

¹³C solid state NMR. ¹³C solid state NMR spectra were obtained with a 4 mm DOTY CP-MAS probe with a Bruker AVANCE III HD spectrometer operating at 125.77 MHz (¹H frequency at 500.13 MHz). The ¹³C CP/TOSS (Cross Polarization with Total Suppression of Spinning Sidebands) spectra were obtained at a sample spinning speed of 7.5 kHz, a ¹H 90° pulse of 5 μs, and a contact time of 2.0 ms, with a ramp pulse on the ¹H channel. Spectral acquisition employed *ca.* 2500 scans with a recycle delay of 1 s, along with a 50 kHz SPINAL-64 decoupling sequence. ¹³C NMR chemical shifts were referenced externally to adamantane at 38.48 ppm *via* the low field signal.

FT-IR spectroscopy. The FT-IR spectra were acquired with a Bio-Rad FTS-40 (Bio-Rad Laboratories, Inc., USA) in reflectance mode using the Kubelka–Munk method. Powdered samples were mixed in a 1 : 10 ratio with KBr (IR-Grade). The diffuse reflectance infrared spectra were measured at 23 °C over a spectral range of 4000–400 cm⁻¹ with a resolution of 4 cm⁻¹. 128 scans were recorded, where a background spectral correction (KBr) was applied.

Thermogravimetric analysis (TGA). The weight loss profiles were obtained with a Q50 TA Instruments thermogravimetric analyser (TA Instruments, USA), the samples were placed in an open aluminium pan under in a N₂ gas atmosphere, which was equilibrated at 30 °C for 1 min and then heated to 500 °C at a rate of 10 °C min⁻¹.

Adsorption studies. For the equilibrium studies, 10 mL of dibasic (pH 8.5) or mono-basic (pH 4.75) potassium phosphate solution were added to one pellet (*ca.* 40 mg) in a 4 DRAM vial. The vials were placed on a Scilogex SK-0330-Pro shaker and shaken for *ca.* 18 h at 220 rpm. The adsorption capacity was calculated with eqn (1):

$$q_e = \frac{C_0 - C_e}{m} \times V \qquad (1)$$

To calculate the equilibrium adsorption capacity, the Sips isotherm model was used according to eqn (2):[36–38]

$$q_e = \frac{Q_m (K_a C_{eq})^{\frac{1}{n_S}}}{1 + (K_a C_{eq})^{\frac{1}{n_S}}} \qquad (2)$$

Q_m represents the maximum monolayer adsorption capacity, K_a is the equilibrium adsorption constant, and q_e is the adsorption capacity at equilibrium. The heterogeneity factor (n_S) describes the nature of the adsorption sites. As the value of n_S approaches 1, the Sips isotherm accounts for Langmuir isotherm behaviour. The level of P_i in the aqueous solution was determined through the vanadate–molybdate reagent (after 20 min development time).[39] Absorbance was measured *via* a Thermo Scientific Spectronic 200E (Waltham, MA, USA) at 420 nm.

Results and discussion

Characterisation

¹³C solid state NMR spectroscopy. Solids NMR spectroscopy was used to study the chemical environment of the ¹³C nuclei within the composites (*cf.* Fig. 2).

The composite formed from oat hulls and chitosan without any NaOH-washing step shows the characteristic carbohydrate fraction between 120–50 ppm, which overlaps with the chitosan carbohydrate pattern. The –CH₃ of the acetyl group for chitosan is observed near 25 ppm. Another signal at 175 ppm, also relates to the carbonyl signature of chitosan, due to the acetyl-moiety, where *ca.* 82% of the biopolymer is deacetylated. Additionally, some remaining lignins and other aromatic constituents are noted between 160–120 ppm in Oh50 and also for Oh50–ECH to a lesser extent. However, these components are mostly removed during the NaOH-washing steps (Oh50–NaOH/Oh50–ECH). The increased peak intensity in Oh50–Furfural in this particular region is posited to originate from the incorporated furfuryl- and pyridinium-moieties. The remaining furfuryl-moieties were
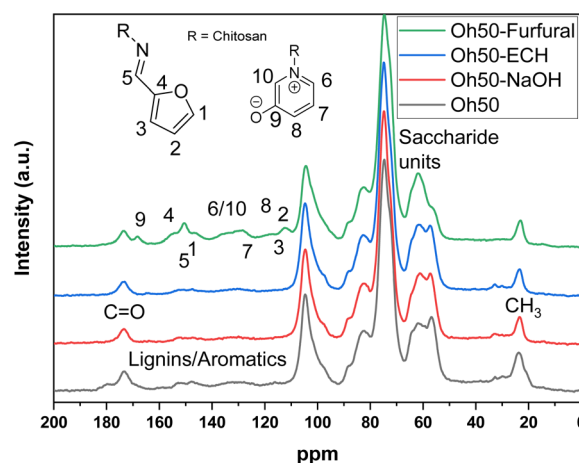

Fig. 2 ¹³C solid state NMR spectra of the unmodified oat hull composite (Oh50), the NaOH washed composite (Oh50–NaOH), the EPH crosslinked composite (Oh50–ECH) and furfuryl-modified composite (Oh50–Furfural).

assigned to signatures near 165–140 ppm and 120–110 ppm, while C9 (170 ppm, stemming for the deprotonated OH-group in the zwitterion form) and C6, C7, C10 in the 140–130 ppm, with C8 potentially overlapping near 120 ppm.[31,35] The reaction proceeds in two distinct steps, with an imine-linkage formed between chitosan and furfural, while ring-opening and closure is organo-catalysed *via* HCOOH to form the pyridinium cation (*cf.* Scheme 1).

TGA. Thermogravimetric profiles can be used to detect changes in decomposition profiles with temperature and can be used to infer compositional variations due to effects of synthetic modification on such biomaterials. To gain insight on the role of chemical modification, the (derivative) weight loss profiles of the precursors and prepared pellets were obtained (*cf.* Fig. 3).

Kaolinite as a starting material does not show any appreciable water content or decomposition events below 400 °C. The other starting materials and composites show evidence of water loss below 100 °C. Raw oat hulls have two thermal events with peak maxima at 291 °C and 336 °C, while chitosan shows a single major peak at 305 °C.[20,40] The early thermal event for the oat hulls can be attributed to its high hemicellulose content, where it decomposes at elevated temperatures. Lignins may also decompose at temperatures near 350 °C. In the composite materials, the first event is shifted to 300 °C, whereas the second event is shifted to an elevated value near 340 °C, except Oh50–Furfural, which has a temperature shift to 355 °C. According to the lower derivative weight loss at *ca.* 330–355 °C, the cellulosic content was lower compared to raw oat hulls and the furfuryl-modified composites show an additional shift and decrease in the derivative weight loss, indicating an elevated content of aromatic components *versus* the other composites, albeit to a lesser degree. Interestingly, the absolute weight loss (*cf.* Fig. 2B) is lowest for the furfural-modified systems, whereas ECH-crosslinking alone did not enhance the thermal stability of the composites. The incorporation of aromatic moieties along furfuryl-groups that possess ionic groups account for the greater thermal stability up to 500 °C.

IR. IR spectroscopy was used to detect the characteristic vibrational bands of the composites, along with the presence or absence of key functional groups. A potential shift in frequency or band broadening may indicate association between the respective functional groups (*cf.* Fig. 4).

The IR bands of kaolinite can be observed for all composites, verifying its presence. IR band broadening occurs near 3500 cm^{-1} and 2880 cm^{-1} that signifies potential H-bonding through OH-groups (and amine groups) within the structure between Oh and Chi, as well as kaolinite.[19,41] The characteristic N–H bend is observed at *ca.* 1663 cm^{-1} for all composites, while an additional sharp band at 1650 cm^{-1} appeared in the Oh50–Furfural system. This supports the presence of a C=C functional group due to the furfuryl moieties.[42] A sharp band around 1564 cm^{-1} may also indicate the presence of aromatic C–C stretching in Oh50–Furfural, originating from the pyridinium moieties.[43] The band at 1502 cm^{-1} only appears for the Oh50–Furfural system, which was assigned to C–C stretching from the aromatic rings. All composites show further evidence of the C–O–C stretch from polysaccharides *ca.* 1150–1000 cm^{-1}. Additionally, the alkane band (C–H) at 752 cm^{-1} is sharper in the Oh50–Furfural *versus* Oh50–ECH, revealing low crosslinker content. These small variations in characteristic bands further indicate that only a part of the available moieties (amine) are modified through furfural. It can be inferred that the pellet surface *versus* the core of composite undergoes effective modification.
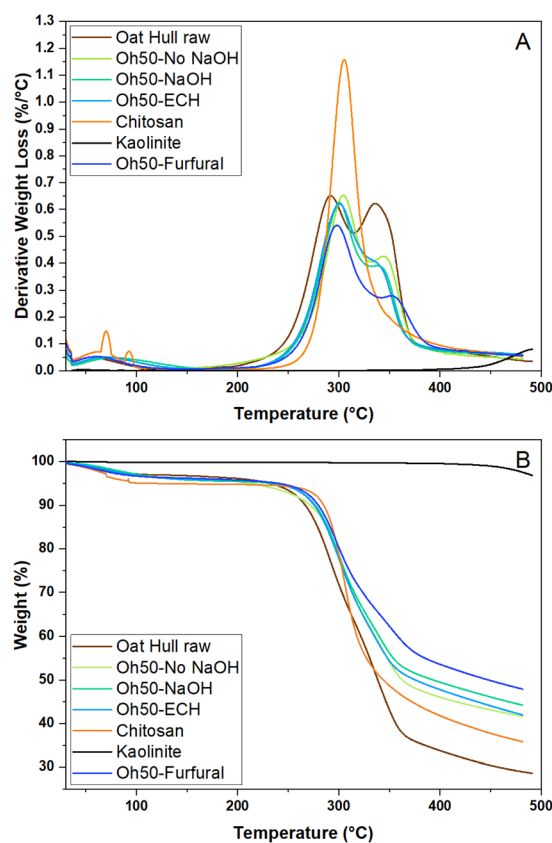

Fig. 3 TGA of all components (starting materials) as well as the four prepared composites with derivative weight loss (A) and weight loss profiles in % (B).
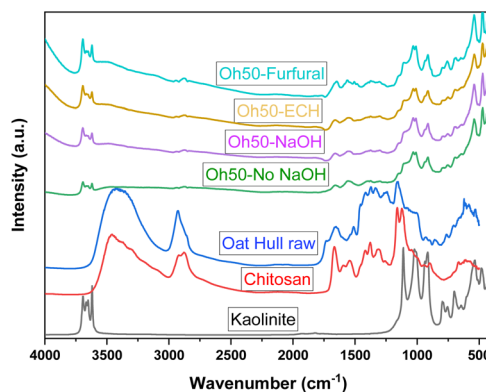

Fig. 4 IR of the starting materials and four types of biomass composites.

Phosphate adsorption

To evaluate the effect of the synthetic modification, adsorption isotherms can be used to assess the change in structural and surface chemical properties *via* the adsorption capacity. Of note, unmodified and non-crosslinked pellet composites were used as benchmarks to assess the effects of NaOH-washing, crosslinking and furfural-modification of the pellet systems.

Adsorption at pH 4.75. In contrast to powdered materials, crosslinked and pelletized adsorbents are expected to have significantly decreased adsorption capacities. This relates to attenuated surface accessible adsorption sites due to steric effects of the biopolymer network (*cf.* Fig. 5).

As expected, the unmodified chitosan pellets that contain fully protonated amine groups, where acetate as the counterion revealed the highest adsorption capacity (*cf.* Table 1 for the adsorption capacity at pH 4.75 and pH 8.5).

Chitosan pellets that were washed with NaOH showed slightly greater adsorption capacity at higher orthophosphate levels, most likely due to protonation. While a maximum adsorption capacity of *ca.* 14 mg g^{-1} at elevated concentrations could be reached with unmodified pellets, these concentrations are rarely environmentally relevant, where the orthophosphate concentrations generally do not exceed 2–5 mg L^{-1}.[44–47] Herein, the furfural-modified composites exhibit a steep rise at low orthophosphate concentrations comparable or exceeding that of unmodified pellets. Notably, the NaOH and ECH modified pellet systems did not display appreciable adsorption at all for such environmentally relevant conditions.

Adsorption at pH 8.5. To evaluate the role of pH of the solution to enable sufficient phosphate uptake, slightly basic conditions were employed (*cf.* Fig. 6 for the adsorption isotherms and Table 1 for uptake capacity).

Only the unmodified and furfural-modified pellets showed an appreciable phosphate uptake, albeit reduced when compared to pH 4.75. Similar to orthophosphate adsorption at pH 8.5, the furfural-modified composites exhibit a steep rise

Table 1 Adsorption capacity at equilibrium of orthophosphate at pH 4.75 and pH 8.5 with various oat hull composites for the Sips isotherm model

	pH 4.75			pH 8.5		
	Q_e (mg g^{-1})	n_S	R^2	Q_e (mg g^{-1})	n_S	R^2
Oh50	13.9	2.0	0.96	6.2	9.9	0.94
Oh50–NaOH	6.1	3.2	0.96	—	—	—
Oh50–ECH	4.1	12.0	0.88	—	—	—
Oh50–Furfural	4.9	1.0	0.93	1.1	40.7	0.69

and suddenly plateau at low orthophosphate concentrations, suggesting the beneficial effect of the synthetic modification, in contrast to sole modification of composites with crosslinking.

When comparing the adsorption of orthophosphate at both pH conditions, the adsorption capacity was roughly doubled at pH 4.75 for Oh50 and Oh50–Furfural. At pH 8.5, Oh50–NaOH and Oh50–ECH did not reveal appreciable adsorption, which only began to adsorb orthophosphate at pH 4.75 and concentrations above 75–100 mg L^{-1}. It is therefore purported, that a positive surface charge was imbued onto chitosan at acidic pH. Therefore, electrostatic interactions between adsorbate and adsorbent govern the adsorption process.[47,48] Priya *et al.* provided an overview of selected materials with their orthophosphate adsorption capacity (see Table 2) at variable conditions.[48]

The maximum adsorption capacity is reached at even low concentrations for environmentally applicable concentrations. In contrast to typical chitosan-based adsorbents, the surface modification also afforded appreciable adsorption (*ca.* 1 mg g^{-1}) onto the prepared pelletized composites at slightly alkaline conditions, obviating pH adjustment to meet optimal conditions.

The inherent benefit of the proposed valorization route is the sustainably sourced raw materials from sugars (furfural),
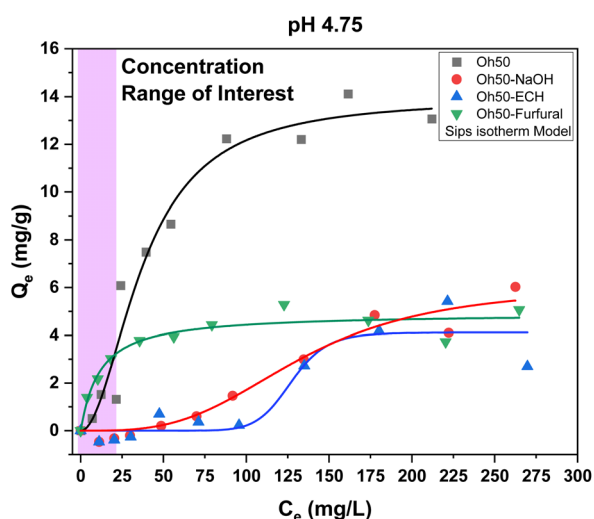

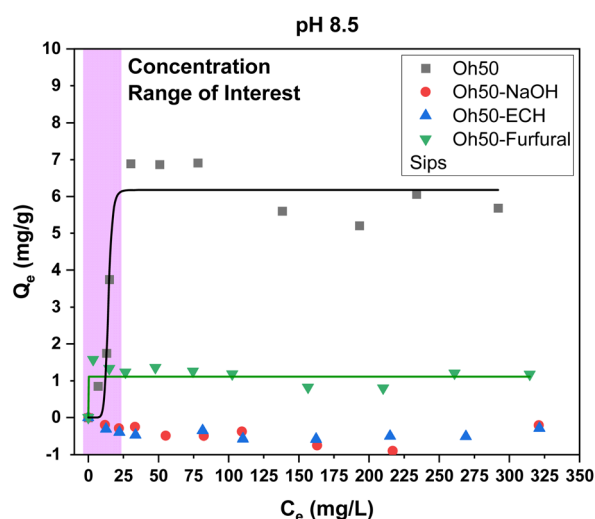**Fig. 5** Phosphate adsorption isotherms at pH 4.75 (monobasic potassium phosphate).

Fig. 6 Phosphate adsorption isotherms at pH 8.5 (dibasic potassium phosphate).

Table 2 Selected examples of adsorbents for orthophosphate capture at variable conditions (pH and concentration)

Adsorbent materials	Q_e (mg g^{-1})	Concentration range (mg L^{-1})	pH
Fe-zeolite-A[49]	18.75	4.725	5
Magnetic Fe-oxide[50]	10.85	2–20	2–6
Iron-modified biochar[51]	2–3	0–100	6–5
MIL-101(Al)-CS[52]	49.8	30	3–10
Chitosan–La beads[53]	107.7	50	4
SP-Zr–La[54]	23.5	30	3
Fe(OH)$_3$@CNF[55]	142.86	10	4.5
Oh50–Furfural (this study)	4.9/1.1	0–300	4.75/8.5

chitosan and under-utilised oat hull agro-waste that otherwise shows limited applicability. This strategy offers accessible and affordable preparation of pelletized adsorbents, which are amenable as slow-release fertilizer carriers, in contrast with inorganic phosphate fertilizer. The high biomass content of the composites lend to their utility as amendment materials for addressing food and water security in agricultural applications.[51,56,57]

Conclusions

The goal of this study was the valorization of oat hulls through composite formation that combines synthetic modification of chitosan *via* functionalization with pyridinium-moieties to provide enhanced adsorption of orthophosphate. Oat hull composites typically show low intrinsic stability in aqueous media, which necessitates crosslinking and potential chemical modification that counters the hydrophilic character of the biomass. In turn, alteration of the hydrophilic character by removal of polar groups such as –OH can yield attenuated adsorption capacity. The adsorbent characterisation *via* ^{13}C NMR spectroscopy for Oh50–Furfural showed that a mixture of imine-linked furfuryl- and pyridinium moieties are attached to the surface sites of chitosan. The yield (pyridinium) could not be quantified accurately but was estimated to be near 30%. The acetylation degree of *ca.* 18% may have limited the yield through reducing the number of active amine sites in chitosan. The modified composites that contain Oh50–Furfural show decreased phosphate adsorption properties of *ca.* 70% compared to Oh50. Oh50 displays low stability in aqueous solution with greater ionic strength, which results in enhanced adsorption properties for Oh50, as compared with Oh50–NaOH and Oh50–ECH.

The adsorption capacity of Oh50–Furfural composite was estimated as 1.1 mg g^{-1} at pH 8.5 while Oh50–NaOH and Oh50–ECH did not reveal any notable orthophosphate uptake. At pH 4.75, the adsorption capacity was 4.9 mg g^{-1} for the Oh50–Furfural composite, which exceeds the uptake capacity of the crosslinked pellets for Oh50–ECH (4.1 mg g^{-1}). Notably, the maximum adsorption capacity reaches a plateau at less than 50 mg L^{-1}, with appreciable adsorption at environmentally relevant concentrations (up to 5 mg L^{-1}). This study relies on sustainable and readily available agro-waste (oat hulls) and sustainably sourced organic precursors (*i.e.*, furfural from sugars), which precludes the use of petrochemicals in the adsorbent design, further aligning with the UN SDG 12 for responsible consumption and production of chemical products in addition to other UN SDGs (goals-2, -6, & -12). Further research will explore alternatives to energy intensive synthesis that requires multi-day synthesis under reflux conditions to develop an alternate strategy that embodies principles of green chemistry. Furthermore, a crucial aspect for continued research is an improved conversion of the furfuryl-moieties into pyridinium-moieties for increased adsorption efficiency through exploring alternative synthetic approaches (*e.g.*, microwave synthesis). Nevertheless, this study provides support for the *proof-of-concept* that chitosan within a physical blend along with ECH crosslinking can be functionalized with pyridinium cations that extends beyond previous starch-based composites.[58] This type of modification reported herein results in improved adsorption properties through a green strategy using sustainably sourced precursors.

Data availability

No data was used for the research described in the article.

Author contributions

B. G. K. S: writing, conceptualisation & materials preparation and characterization, experimental & data analysis, editing; L. D. W: funding acquisition, writing – review & editing, supervision and funding.

Conflicts of interest

The authors declare that they have no known competing financial interests or personal relationships that could have appeared to influence the work reported in this paper.

Acknowledgements

Notes and references

1 UNESCO, *Water Security and the Sustainable Development Goals*, https://sdgs.un.org/goals, accessed July 27, 2023.

2 T. K. M. Prashantha Kumar, T. R. Mandlimath, P. Sangeetha, S. K. Revathi and S. K. Ashok Kumar, *Environ. Chem. Lett.*, 2018, **16**, 389–400.

3 H. K. Agbovi, L. D. Wilson and L. G. Tabil, *Ind. Eng. Chem. Res.*, 2017, **56**, 37–46.

4 S. P.-M. Ung and C.-J. Li, *RSC Sustainability*, 2023, **1**, 11–37.

5 P. Hlabela, J. Maree and D. Bruinsma, *Mine Water Environ.*, 2007, **26**, 14–22.

6 D. J. Bosman, J. A. Clayton, J. P. Maree and C. J. L. Adlem, *Int. J. Mine Water*, 1990, **9**, 149–163.

7 B. Peng, Z. Yao, X. Wang, M. Crombeen, D. G. Sweeney and K. C. Tam, *Green Energy Environ.*, 2020, **5**, 37–49.

8 C. Xue and L. D. Wilson, *J. Compos. Sci.*, 2021, **5**, 160.

9 K. O. Iwuozor, J. O. Ighalo, E. C. Emenike, L. A. Ogunfowora and C. A. Igwegbe, *Curr. Res. Green Sustainable Chem.*, 2021, **4**, 100179.

10 S. Fatullayeva, D. Tagiyev, N. Zeynalov, S. Mammadova and E. Aliyeva, *J. Polym. Res.*, 2022, **29**, 259.

11 J. Wang and S. Zhuang, *J. Cleaner Prod.*, 2022, **355**, 131825.

12 C. K. S. Pillai, W. Paul and C. P. Sharma, *Prog. Polym. Sci.*, 2009, **34**, 641–678.

13 M. Bilal, I. Ihsanullah, M. U. Hassan Shah, A. V. Bhaskar Reddy and T. M. Aminabhavi, *J. Environ. Manage.*, 2022, **321**, 115981.

14 J. Hu, L. Zhao, J. Luo, H. Gong and N. Zhu, *J. Hazard. Mater.*, 2022, **438**, 129437.

15 M. El Wali, S. R. Golroudbary and A. Kraslawski, *Sci. Total Environ.*, 2021, **777**, 146060.

16 H. N. Hamad and S. Idrus, *Polymers*, 2022, **14**, 783.

17 M. S. Karunarathna and R. C. Smith, *Sustainability*, 2020, **12**, 734.

18 M. V. Barros, R. Salvador, A. C. de Francisco and C. M. Piekarski, *Renewable Sustainable Energy Rev.*, 2020, **131**, 109958.

19 M. H. Mohamed, I. A. Udoetok, M. Solgi, B. G. K. Steiger, Z. Zhou and L. D. Wilson, *Front. Water*, 2022, **4**, 739492.

20 B. G. K. Steiger, Z. Zhou, Y. A. Anisimov, R. W. Evitts and L. D. Wilson, *Ind. Crops Prod.*, 2023, **191**, 115913.

21 M. H. Mohamed, I. A. Udoetok and L. D. Wilson, *J. Compos. Sci.*, 2020, **4**, 15.

22 V. L. Triana-Guzmán, Y. Ruiz-Cruz, E. L. Romero-Peñaloza, H. F. Zuluaga-Corrales and M. N. Chaur-Valencia, *Rev. Fac. Ing., Univ. Antioquia*, 2018, 34–43.

23 Y. A. Anisimov, B. G. K. Steiger, D. E. Cree and L. D. Wilson, *J. Compos. Sci.*, 2023, **7**, 100.

24 S. Jiang, X. Wu, S. Du, Q. Wang and D. Han, *Water*, 2022, **14**, 2813.

25 M. Solgi, B. G. K. Steiger and L. D. Wilson, *Separations*, 2023, **10**, 262.

26 S. Despax, C. Maurer, B. Estrine, J. Le Bras, N. Hoffmann, S. Marinkovic and J. Muzart, *Catal. Commun.*, 2014, **51**, 5–9.

27 Z. Yuan, C. Xu, S. Cheng and M. Leitch, *Carbohydr. Res.*, 2011, **346**, 2019–2023.

28 T. S. Hansen, J. Mielby and A. Riisager, *Green Chem.*, 2011, **13**, 109–114.

29 P. Wrigstedt, J. Keskiväli, J. E. Perea-Buceta and T. Repo, *ChemCatChem*, 2017, **9**, 4244–4255.

30 A. A. Rosatella, S. P. Simeonov, R. F. M. Frade and C. A. M. Afonso, *Green Chem.*, 2011, **13**, 754.

31 S. Kirchhecker, S. Tröger-Müller, S. Bake, M. Antonietti, A. Taubert and D. Esposito, *Green Chem.*, 2015, **17**, 4151–4156.

32 M. Y. Lui, C. Y. Y. Wong, A. W.-T. Choi, Y. F. Mui, L. Qi and I. T. Horváth, *ACS Sustainable Chem. Eng.*, 2019, **7**, 17799–17807.

33 K. C. Badgujar, L. D. Wilson and B. M. Bhanage, *Renewable Sustainable Energy Rev.*, 2019, **102**, 266–284.

34 C. Hermouet, R. Garnier, M.-L. Efthymiou and P.-E. Fournier, *Am. J. Ind. Med.*, 1996, **30**, 759–764.

35 S. Sowmiah, L. F. Veiros, J. M. S. S. Esperança, L. P. N. Rebelo and C. A. M. Afonso, *Org. Lett.*, 2015, **17**, 5244–5247.

36 R. Sips, *J. Chem. Phys.*, 1948, **16**, 490–495.

37 S. Kalam, S. A. Abu-Khamsin, M. S. Kamal and S. Patil, *ACS Omega*, 2021, **6**, 32342–32348.

38 B. G. K. Steiger and L. D. Wilson, *Surfaces*, 2022, **5**, 429–444.

39 H. K. Agbovi and L. D. Wilson, *Carbohydr. Polym.*, 2018, **189**, 360–370.

40 T. Emiola-Sadiq, L. Zhang and A. K. Dalai, *ACS Omega*, 2021, **6**, 22233–22247.

41 C. Paluszkiewicz, E. Stodolak, M. Hasik and M. Blazewicz, *Spectrochim. Acta, Part A*, 2011, **79**, 784–788.

42 J. Cui, Y. Sun, L. Wang, Q. Miao, W. Tan and Z. Guo, *Mar. Drugs*, 2022, **20**, 688.

43 S. Omidi and A. Kakanejadifard, *Carbohydr. Polym.*, 2019, **208**, 477–485.

44 H. K. Agbovi and L. D. Wilson, in *Natural Polymers-Based Green Adsorbents for Water Treatment*, Elsevier, 2021, pp. 1–51.

45 P. J. McGinn, K. C. Park, G. Robertson, L. Scoles, W. Ma and D. Singh, *Algal Res.*, 2019, **38**, 101418.

46 M. J. Waiser, V. Tumber and J. Holm, *Environ. Toxicol. Chem.*, 2011, **30**, 496–507.

47 L. N. Pincus, H. E. Rudel, P. V. Petrović, S. Gupta, P. Westerhoff, C. L. Muhich and J. B. Zimmerman, *Environ. Sci. Technol.*, 2020, **54**, 9769–9790.

48 E. Priya, S. Kumar, C. Verma, S. Sarkar and P. K. Maji, *J. Water Process Eng.*, 2022, **49**, 103159.

49 M. Saifuddin, J. Bae and K. S. Kim, *Water Res.*, 2019, **158**, 246–256.

50 S.-Y. Yoon, C.-G. Lee, J.-A. Park, J.-H. Kim, S.-B. Kim, S.-H. Lee and J.-W. Choi, *Chem. Eng. J.*, 2014, **236**, 341–347.

51 D. G. Strawn, A. R. Crump, D. Peak, M. Garcia-Perez and G. Möller, *PLoS Water*, 2023, **2**, e0000092.

52 S. Zhang, J. Ding and D. Tian, *J. Solid State Chem.*, 2022, **306**, 122709.

53 K. Y. Koh, Z. Chen, S. Zhang and J. P. Chen, *Chemosphere*, 2022, **286**, 131458.

54 W. Du, Y. Li, X. Xu, Y. Shang, B. Gao and Q. Yue, *J. Colloid Interface Sci.*, 2019, **533**, 692–699.

55 G. Cui, M. Liu, Y. Chen, W. Zhang and J. Zhao, *Carbohydr. Polym.*, 2016, **154**, 40–47.

56 Q. Yin, B. Zhang, R. Wang and Z. Zhao, *Environ. Sci. Pollut. Res.*, 2017, **24**, 26297–26309.

57 A. Adamczuk, M. Kercheva, M. Hristova and G. Jozefaciuk, *Materials*, 2021, **14**, 7724.

58 A. H. Karoyo, L. Dehabadi and L. D. Wilson, *ACS Sustainable Chem. Eng.*, 2018, **6**, 4603–4613.